CHEMICAL ENGINEERING TRANSACTIONS
VOL. 68, 2018
A publication of AIDIC
The Italian Association of Chemical Engineering
Online at www.aidic.it/cet
Guest Editors: Selena Sironi, Laura Capelli

ISBN 978-88-95608-65-5; **ISSN** 2283-9216

Cu-Graphene Nanostructures for Low Concentration CH3SH Removal

Maria Sarno*, Eleonora Ponticorvo

Department of Industrial Engineering and Centre NANO_MATES University of Salerno, Via Giovanni Paolo II ,132 - 84084 Fisciano (SA), Italy
eponticorvo@unisa.it

Mercaptans are molecules with high volatility, responsible for unpleasant odours. They have a very low olfactory threshold, e.g. for CH_3SH of ~0.39 ppbv. In this paper, copper oxide nanoparticles supported on graphene were synthesized for the removal of low-concentration CH_3SH (5 ppm). That results show that the humidity has a significant impact on the elimination of odors. The adsorption ability grows at increasing conditions of relative humidity (RH). The adsorption capacity at RH = 80 % is 2 or 5 times higher than that shown at RH = 4 %. The surface of CuO nanoparticles is highly responsible for the formation of hydrated complexes that are effective in the acquisition of CH_3SH.

1. Introduction

CH_3SH (methyl mercaptan, methanethiol, MM), that is a colorless gas, is a typical sulfur containing volatile organic compounds (VOCs) showing toxicity and threshold of active perception of ~0.39 ppbv (Bashkova et al., 2002). Energy activities (petroleum, natural gas based processes,…), wood industries for the production of papers, some organic processes (paint industries,…) and some activities for environmental remediation (sewage/waste water treatment…) are characterized by this unpleasant smell (Hwang et al., 1995). For disagreeable gas control, catalytic processes (Bashkova et al., 2005; Kumar et al., 2016), absorption (Bashkova et al., 2002; Wang et al., 2017), plasma (Van Durme et al., 2008) and biological (Lebrero et al., 2014) approaches, can be used. Each of these methods offers advantages and disadvantages. For example, catalytic method, that are energy saving and a final disposal process (Vandervaart et al., 1991), suffers from sulfur enriched VOCs deactivation. The co-existence of alcohols, aldehydes, ketones, acetates, alkanes, aromatics, or chlorinated hydrocarbon in the VOCs is responsible for the inefficiency of non-thermal plasma method (Liu et al., 2016). As far as biological method is concerned, it require stable and high concentration of CH_3SH and modulation of the air flow (Lebrero et al., 2014). Moreover, although these processes permits a concentration reduction of CH_3SH (from one hundred ppm to tens of ppm), the resulting exhaust is still unbearable. Therefore, there is an urgent need to find a way to thoroughly remove lower-concentrated CH_3SH emissions and make the exhaust gas completely odorless. To the best of our knowledge, methods of removing low-concentrated CH_3SH (i.e. 1-10 ppm) are scarcely reported.
Porous materials (e.g. activated carbon, metal organic frameworks) are a favourable choice to purify low-concentrated malodour due to the large surface area and abundant adsorption sites (Ma et al., 2016; Weber et al., 2005). Among various transition metals, copper can be doped into many materials and results in positive purgative influence (Zhao et al., 2015). The objective of the present study was to investigate, for the first time, the efficacy of copper/graphene nanostructures for removal of low-concentrated odours. The experiments were performed in an isothermal quartz tube and under steady-state conditions at temperature of 30 °C. CH_3SH was employed as a model odour. The multifunctional nanostructures, obtained by thermolysis of suitable precursors in organic solvent in presence of graphene, were characterized by the combined use of different techniques. Raman Spectroscopy, Transmission Electron Microscopy (TEM) and X-ray diffraction (XRD) were employed.

2. Experimental

The preparation of the nanoparticles (Sarno et al., 2014a; Sarno et al., 2015; Sarno et al., 2016a) was carried out using standard airless procedures and commercially available reagents. Absolute ethanol and hexane were used as received. Benzyl ether (99%), 1,2-hexadecanediol (97%), oleic acid (90%), oleylamine (>70%), copper (II) acetylacetonate were purchased from Aldrich Chemical Co. In particular, $Cu(C_5H_7O_2)_2$ (2 mmol), 1,2-hexadecanediol (10 mmol), oleic acid (6 mmol), oleylamine (6 mmol) and 0.2 g of graphene (Casa et al., 2018) were mixed and magnetically stirred under a nitrogen flow. The mixture was heated to 180 °C for 30 min and then, under a blanket of nitrogen, furtherly heated to reflux (265 °C) for 30 min. The formed black-brown mixture was cooled to room temperature by removing the heat source. Under ambient conditions, ethanol (40 mL) was added to the mixture, and a black material was precipitated and separated via centrifugation. The black product was then dissolved in hexane. Centrifugation (6000 rpm, 10 min) was applied to remove any undispersed residue (Sarno et al., 2016b). The nanohybrid were then precipitated with ethanol, centrifuged (6000 rpm, 10 min) to remove the solvent, and redispersed into hexane. The obtained nanohybrid was named Cu-Graphene in the following. The characterization was obtained by different techniques. Transmission electron microscopy (TEM) images were acquired using a FEI Tecnai electron microscope, equipped with an EDX probe, and operated at 200 KV with a LaB6 filament as source of electrons. Raman spectra were obtained at room temperature with a micro-Raman spectrometer Renishaw inVia with a 514 nm excitation wavelength (laser power 30 mW) in the range 100-3000 cm^{-1}. XRD measurements were performed with a Bruker D8 X-ray diffractometer using CuKα radiation.

The adsorption experiments were carried out in an isothermal quartz tube (bed depth 20 mm, diameter 7 mm) under steady-state conditions at 30 °C (see Scheme 1) at an empty bed residence time of ~ 10 s. The adsorbents (100 mg) were placed in the tube and the gas flow rate through the reactor was 500 ml/min ([CH_3SH] = 5 ppm).The tested sample was pre-humidified with moist air (RH=4 %, 45 %, and 80 % at 30 °C) for 1 h. Relative humidity was analyzed by CENTER-310 humidity temperature meter. The value of CH_3SH "breakthrough" concentration in this study was 0.01 ppm. The time at which the concentration of CH_3SH in the effluent surpassed 0.01 ppm was designated as the "breakthrough time". The concentration of CH_3SH was detected by an electrochemical sensor (Detection Range 0-10 ppm, Sensitivity 0.70 ± 0.15 mA/ppm, Repeatability <±2%signal, Resolution 0.1 ppm). For each sample the breakthrough test was repeated at least twice. A dead time of less than 10 s for our experiments results negligible in comparison with the time of adsorbing. The regeneration of the adsorbent was also studied, exhausted adsorbent (at breakthrough time) was heated to 200 °C in air for 1.5 hour. Then the experiment of adsorption was repeated to test the regenerated adsorbent.

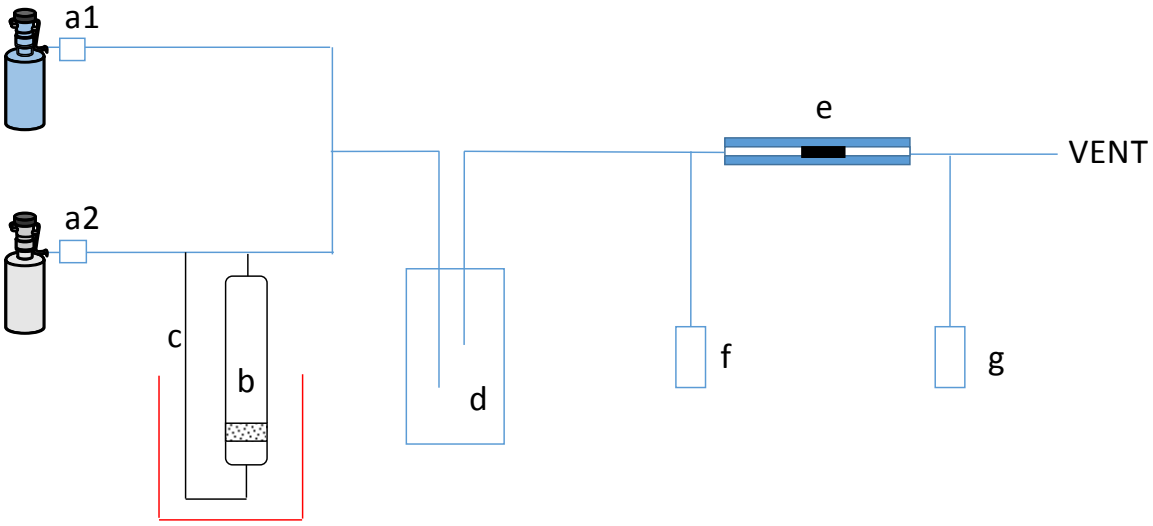

Scheme 1: Schematic representation of apparatus for tests. (a) flow meter, (b) bubbler with sieve plate, (c) water bath thermostat, (d) mixer gas bottle, (e) quartz tube, (f) humidity temperature meter, (g) electrochemical sensor.

3. Results and discussion

Sharp diffraction peaks in the XRD pattern (Figure 1) indicate crystalline structure of CuO (JCPDS 48-1548) formation. The main diffraction peaks of Cu-Graphene belong to CuO. Obviously, the diffraction pattern of the sample is the superposition of both CuO and graphene, which indicates the graphene sheets have been exfoliated from the graphite effectively and the CuO has been incorporated into the graphene sheets successfully. The Raman spectrum of Cu-Graphene nanostructures is shown in Figure 2. It can be seen that, two prominent peaks at about 1590 cm^{-1} and 1320 cm^{-1}, corresponding to the well documented G band and D band, respectively, are observed in the Raman spectra of these samples (Sarno et al., 2014a; Sarno et al., 2014b). It is well known that the G band is usually assigned to the E_{2g} symmetry of sp^2 carbon atoms, while D band is a breathing mode of the A_{1g} symmetry (Jeong et al., 2008). The D band is associated with structural defects and disorder, the intensity ratio of the D band to G band (I_D/I_G) is considered as an indicator of the disorder (Scherrer, 1918). Moreover, the peaks at Raman shift lower than 700 cm^{-1} can be ascribed to CuO (Pendashteh et al., 2013).

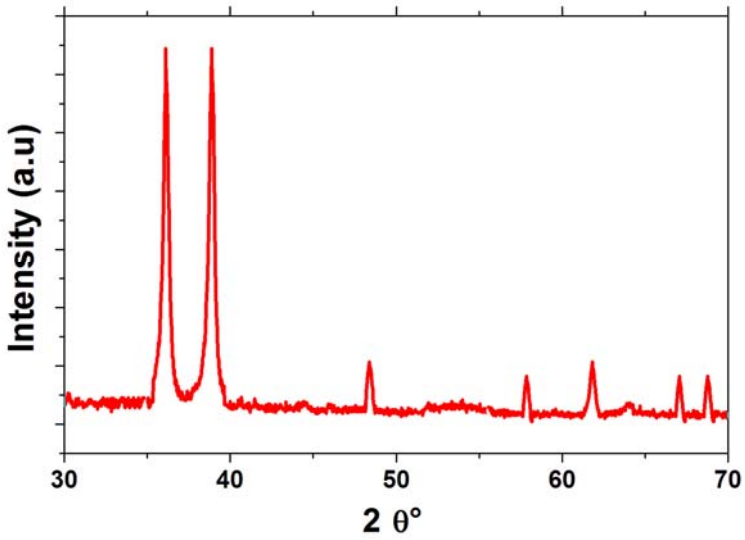

Figure 1: XRD diffraction pattern of Cu-Graphene.

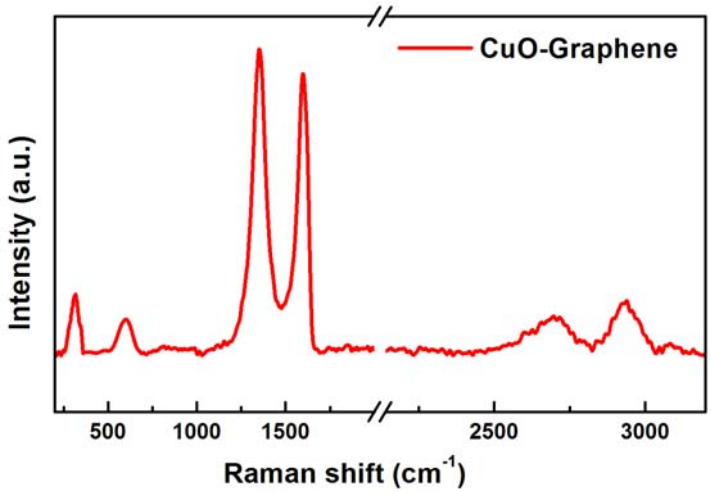

Figure 2: Raman spectrum of Cu-Graphene.

TEM image, carried out to provide insights into the morphology of Cu-Graphene nanohybrid, is reported in Figure 3. Figure 3 shows a typical image of the product, that consists of 10 nm to 40 nm nanoparticles, dispersed on graphene preventing agglomeration. The TEM image reveals that the CuO nanoparticles are attached to the graphene sheets, even after the ultrasonication used to disperse the nanohybrid for TEM characterization.

The result of CH_3SH removal in the gas phase is presented in Figure 4. In particular, the breakthrough time for CH_3SH adsorption in Cu-Graphene is recorded. In Figure 4 the different adsorption capacities of CH_3SH, in various conditions of relative humidity and at a temperature of 30 °C, are shown. The adsorption ability grows at increasing conditions of relative humidity. Especially, the adsorption capacity at RH = 80 % (~ 20 mg/g) is 2 or 5 times higher than that shown at RH = 4 %. Thus, water facilitates the CH_3SH adsorption by affecting copper species of Cu-Graphene. The adsorption ability of the nanohybrid was found dependent on the water humidity, indicating that the surface groups on CuO nanoparticles form hydrated complexes that are highly effective in the acquisition of CH_3SH. This is probably due to the Cu -3d empty orbit. Although CH_3SH must compete with water to have access to the adsorption sites, its strong chelation capacity, between -SH group and Cu (II), prevails.

Recovery of adsorbents is important for the re-usage and determines the cost of the adsorbent. CuO doped graphene samples were heated to 200 °C for 1.5 h before they were reused in a further round of adsorption. In particular, the sample is applied for 7 successive runs and the adsorption efficiency so obtained reported in Figure 5. After seven adsorption-desorption cycles, the adsorbability of Cu-Graphene has a slight change, demonstrating that the Cu-Graphene exhibits good recyclability, recording a maximum deviation from the initial breakthrough time of ~ 4%.

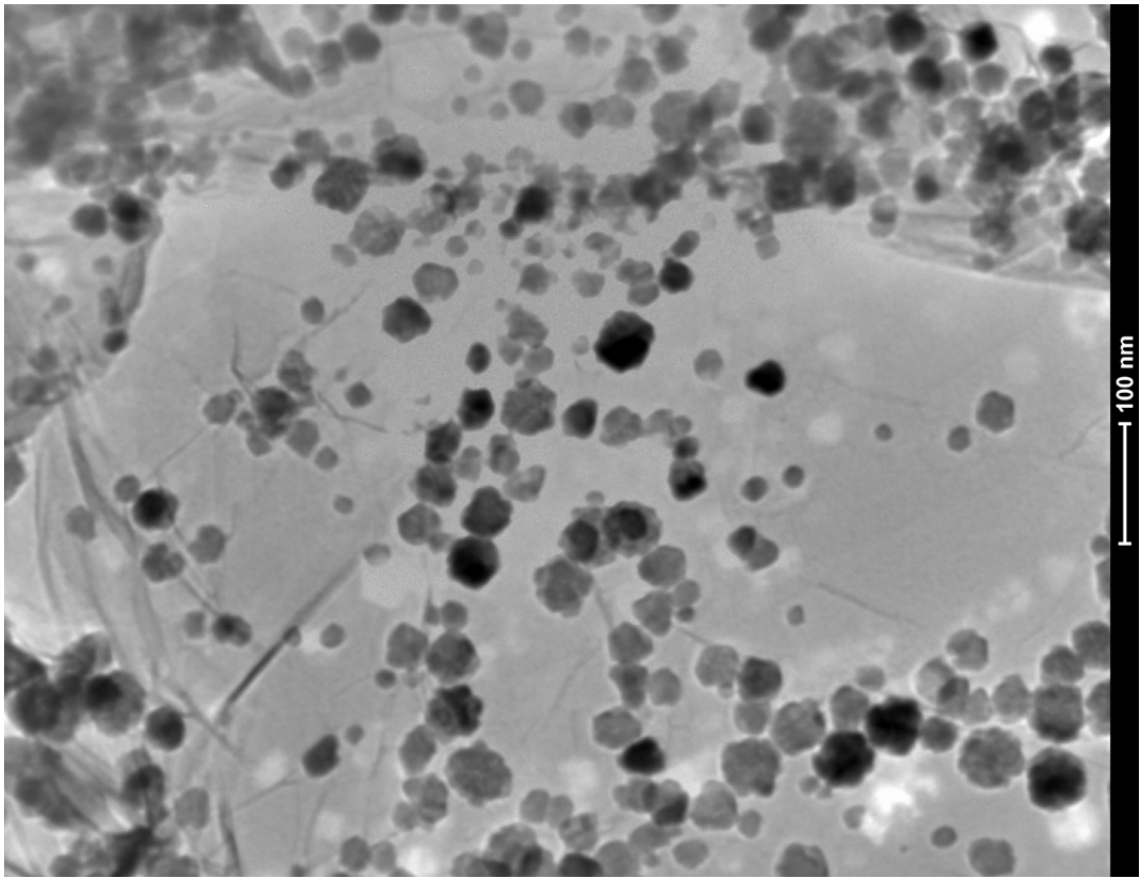

Figure 3: TEM images of Cu-Graphene (a, b).

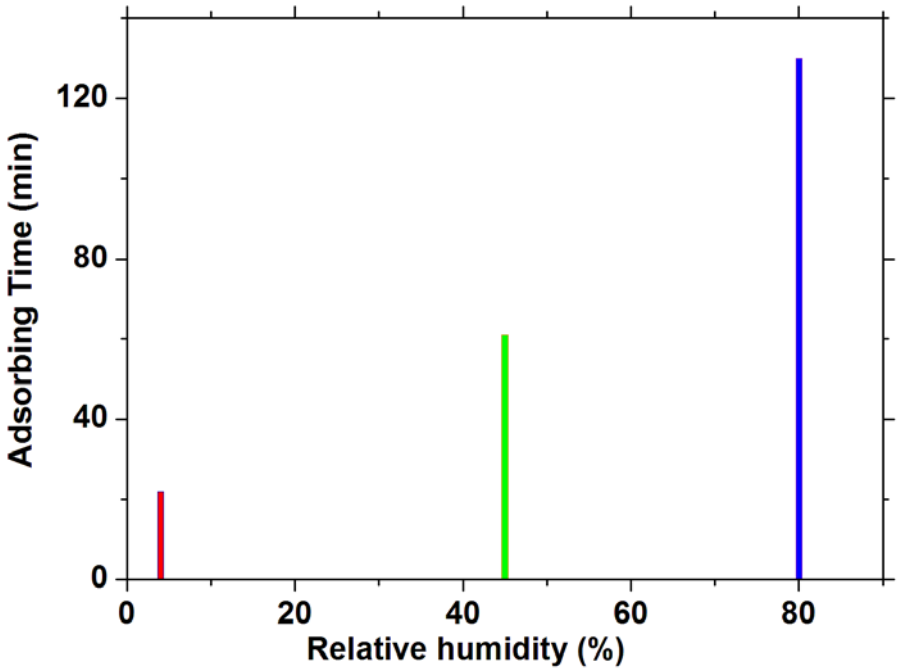

Figure 4: Adsorption time of CH_3SH at various relative humidities (30 °C). The adsorption time means that CH_3SH is totally adsorbed by samples in this period.

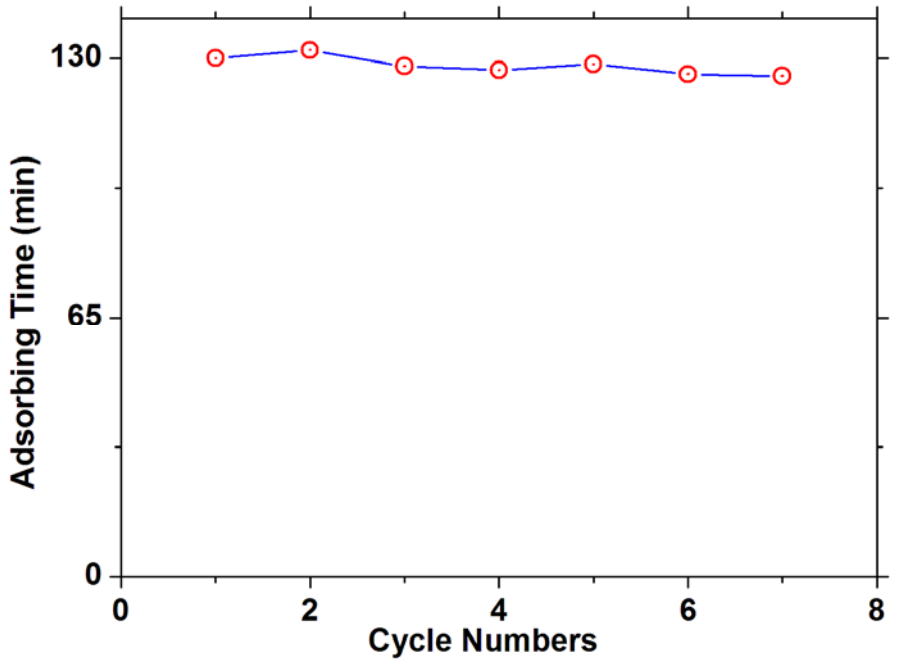

Figure 5: Adsorption-desorption recyclability.

4. Conclusions

Nanoparticles of 10 nm to 40 nm diameters, dispersed on graphene preventing agglomeration, have been prepared by a bottom-up synthetic approach. The TEM image reveals that the CuO nanoparticles are attached to the graphene sheets, even after the ultrasonication used to disperse the nanohybrid for TEM characterization.

The nanomaterial produced in the present study can also be applied to atmospheric control for the removal of thiol compounds from air.

References

Bashkova S., Bagreev A., Bandosz T.J., 2002, Adsorption of Methyl Mercaptan on Activated Carbons, Environmental Science & Technology, 36, 2777-2782.

Bashkova S., Bagreev A., Bandosz T.J.,2005, Catalytic properties of activated carbon surface in the process of adsorption/oxidation of methyl mercaptan, Catalysis Today, 99, 323-328.

Casa M., Sarno M., Liguori, R., Cirillo C., Rubino A., Bezzeccheri E., Liu, J., Ciambelli P., 2018, Conductive Adhesive Based on Mussel-Inspired Graphene Decoration with Silver Nanoparticles, Journal Of Nanoscience And Nanotechnology, 18, 1176-1185.

Hwang Y., Matsuo T., Hanaki K., Suzuki N.,1995, Identification and quantification of sulfur and nitrogen containing odorous compounds in wastewater, Water Research, 29, 711-718.

Jeong S., Woo K., Kim D., Lim S., Kim J.S., Shin H., Xia Y., Moon J., 2008, Advanced Functional Materials, 18, 679–686.

Kumar A., Smith M.A., Kamasamudram K., Currier N.W., Yezerets A., 2016, Chemical deSOx: an effective way to recover Cu-zeolite SCR catalysts from sulfur poisoning, Catalysis Today, 267, 10–16.

Lebrero R., Celina Gondim A., Perez R., Garcia-Encina P.A., Munoz R., 2014, Comparative assessment of a biofilter, a biotrickling filter and a hollow fiber membrane bioreactor for odor treatment in wastewater treatment plants, Water Research, 49, 339-350.

Liu H.D., Li W.M., Ma X., Chen Y.F., 2016, Absorbing Low-Concentration Mercaptan with Active Carbon Doped by Copper, Chinese Journal of Inorganic Chemistry, 32, 1026-1032.

Ma X., Liu H., Li W., Peng S., Chen Y., 2016, Reactive adsorption of low concentration methyl mercaptan on a Cu-based MOF with controllable size and shape , RSC Advances, 6, 96997-97003.

Pendashteh A., Mousavi M.F., Rahmanifar M.S.,2013, Fabrication of anchored copper oxide nanoparticles on graphene oxide nanosheets via an electrostatic coprecipitation and its application as supercapacitor, Electrochimica Acta, 88, 347– 357.

Sarno M., Cirillo C., Ciambelli P., 2014a, Selective graphene covering of monodispersed magnetic nanoparticles, Chemical Engineering Journal, 246, 27-38.

Sarno M., Cirillo C., Ponticorvo E., Ciambelli P., 2015, Synthesis and characterization of FLG/Fe3O4 nanohybrid supercapacitor, Chemical Engineering Transactions, 43, 727-732.

Sarno M., Ponticorvo E., Cirillo C., 2016b, High surface area monodispersed Fe3O4 nanoparticles alone and on physical exfoliated graphite for improved supercapacitors, Journal of Physics and Chemistry of Solids, 99, 138-147.

Sarno M., Ponticorvo E., Cirillo C., Ciambelli P., 2016a, Magnetic nanoparticles for PAHs solid phase extraction, Chemical Engineering Transactions, 47, 313-318.

Sarno, M., Senatore, A., Cirillo, C., Petrone, V., Ciambelli, P., 2014b, Oil lubricant tribological behaviour improvement through dispersion of few layer graphene oxide, Journal of Nanoscience and Nanotechnology, 14, 4960-4968.

Scherrer P., 1918, Bestimmung der Grosse und der Inneren Struktur von Kolloidteilchen Mittels Rontgenstrahlen, Nachrichten von der Gesellschaft der Wissenschaften, Gottingen. Mathematisch-Physikalische Klasse, 98.

Van Durme J., Dewulf J., Leys C., Van Langenhove H., 2008, Combining non-thermal plasma with heterogeneous catalysis in waste gas treatment: A review , Applied Catalysis B: Environmental, 78, 324-333.

Vandervaart D.R., Vatvuk W.M., Wehe A.H., 1991, Thermal and Catalytic Incinerators for the Con- trol of VOCs, Journal of the Air & Waste Management Association, 41, 92-98.

Wang L., Wang X., Ning P., Liu W., Wang F., Ma Y., 2017, Selective adsorption of CH3SH on cobalt-modified activated carbon with low oxygen concentration, Journal of the Taiwan Institute of Chemical Engineers, 75, 156–163.

Weber G., Bellat J.P., Benoit F., Paulin C., Limborg-Noetinger S., Thomas M., 2005, Adsorption Equilibrium of Light Mercaptans on Faujasites, Adsorption, 11, 183-188.

Zhao S., Yi H., Tang X., Gao F., Zhang B., Wang Z., Zuo Y., 2015, Methyl mercaptan removal from gas streams using metal-modified activated carbon, Journal of Cleaner Production, 87, 856-861.